



# Two-component Brownian coagulation: Monte Carlo simulation and process characterization

Haibo Zhao\*, Chuguang Zheng

State Key Laboratory of Coal Combustion, Huazhong University of Science and Technology, Wuhan, 430074 Hubei, China

## ARTICLE INFO

### Article history:

Received 17 November 2010

Accepted 21 April 2011

### Keywords:

Multivariate population balance

Aggregation

Stochastic method

Mixing

Self-preserving

## ABSTRACT

The compositional distribution within aggregates of a given size is essential to the functionality of composite aggregates that are usually enlarged by rapid Brownian coagulation. There is no analytical solution for the process of such two-component systems. Monte Carlo method is an effective numerical approach for two-component coagulation. In this paper, the differentially weighted Monte Carlo method is used to investigate two-component Brownian coagulation, respectively, in the continuum regime, the free-molecular regime and the transition regime. It is found that (1) for Brownian coagulation in the continuum regime and in the free-molecular regime, the mono-variate compositional distribution, i.e., the number density distribution function of one component amount (in the form of volume of the component in aggregates) satisfies self-preserving form the same as particle size distribution in mono-component Brownian coagulation; (2) however, for Brownian coagulation in the transition regime the mono-variate compositional distribution cannot reach self-similarity; and (3) the bivariate compositional distribution, i.e., the combined number density distribution function of two component amounts in the three regimes satisfies a semi self-preserving form. Moreover, other new features inherent to aggregative mixing are also demonstrated; e.g., the degree of mixing between components, which is largely controlled by the initial compositional mass fraction, improves as aggregate size increases.

© 2011 Chinese Society of Particuology and Institute of Process Engineering, Chinese Academy of Sciences. Published by Elsevier B.V. All rights reserved.

## 1. Introduction

Multi-component Brownian coagulation is ubiquitous in nature and in engineering, e.g., nanocomposite ceramic powders ( $\text{Al}_2\text{O}_3/\text{TiO}_2$ ), with special properties such as superconductivity, superparamagnetism, or high catalytic activity, produced through Brownian coagulation from a mixture of nanoparticle precursors of functional molecular-scale monomers (Pratsinis, 1998). Insight into the evolution of compositional distribution is very useful to optimize the synthesis process of nanoparticles while tailoring the functional particles, typically via the gas phase method at high temperature. Brownian coagulation of a two-component non-reactive system is obviously the most basic, and the most important case. Spatially homogeneous two-component coagulation processes are described by the following bivariate population balance equation (PBE) which is an extension of Smoluchowski's equation for one-

component coagulation (Lushnikov, 1976):

$$\begin{aligned} \frac{\partial n(v_x, v_y, t)}{\partial t} = & \frac{1}{2} \int_0^{v_x} \int_0^{v_y} \beta(v_x - v'_x, v_y - v'_y, v'_x, v'_y, t) \\ & \times n(v_x - v'_x, v_y - v'_y, t) n(v'_x, v'_y, t) dv'_x dv'_y \\ & - n(v_x, v_y, t) \int_0^\infty \int_0^\infty \beta(v_x, v_y, v'_x, v'_y, t) \\ & \times n(v'_x, v'_y, t) dv'_x dv'_y. \end{aligned} \quad (1)$$

The underlying nature of Eq. (1) is a two-component coagulation event between particle A of state  $(v_x, v_y)$  and particle B of state  $(v'_x, v'_y)$  to result in a new particle C of state  $(v_x + v'_x, v_y + v'_y)$  and the death of particles A and B. Here  $v_x$  and  $v_y$  are the volume of x-component and y-component, respectively, within an aggregate having volume of  $v_x + v_y$ ;  $n(v_x, v_y, t)$  is the number density function at time  $t$ , such that  $n(v_x, v_y, t) dv_x dv_y$  represents the number concentration of particles in the size range of x-component,  $v_x$  to  $v_x + dv_x$ , and the size range of y-component,  $v_y$  to  $v_y + dv_y$ ;  $\beta(v_x, v_y, v'_x, v'_y, t)$  is the coagulation rate coefficient between par-

\* Corresponding author. Tel.: +86 27 87545526; fax: +86 27 87545526.  
E-mail address: [klinsmannzhb@163.com](mailto:klinsmannzhb@163.com) (H. Zhao).

**Nomenclature**

$C'$	total coagulation rate of a simulation particle, $\text{m}^{-3} \text{s}^{-1}$
$d$	particle diameter of raindrop, $\mu\text{m}$
$m$	particle mass
$M$	total particle mass
$n$	number density function, $\text{m}^{-3}$
$N$	total particle number, $\text{m}^{-3}$
$v$	particle volume
$w$	number weight

**Greek letters**

$\alpha$	multiplicative constant
$\beta$	coagulation kernel, $\text{m}^3/\text{s}$
$\eta$	dimensionless particle volume
$\Psi$	dimensionless particle size distribution
$\tau$	characteristic coagulation time scale

**Subscripts**

0	initial condition
$i, j$	indices of simulation particles
min	minimum value
max	maximum value
$p, q$	a section of compositional distribution
$p$	particles
$x, y$	component style

**Superscripts**

co	continuum regime
fm	free-molecular regime
tr	transition regime

ticles A and B. In this study, the coagulation kernel is considered composition-independent. With respect to Brownian coagulation between particles  $i$  (volume  $v_i$ , diameter  $d_i$  and mass  $m_i$ ) and  $j$  (volume  $v_j$ , diameter  $d_j$  and mass  $m_j$ ), its kernel is characterized by three widely used formulas, depending on the ratio of the mean free path ( $\lambda$ ) of gas molecule to particle radius ( $d/2$ ), that is, the Knudsen number,  $Kn = 2\lambda/d$ .

In the continuum ( $Kn \leq 0.1$ ) and near-continuum ( $0.1 < Kn \leq 1$ ) regime (Friedlander & Wang, 1966):

$$\beta_{ij}^{\text{co}} = \frac{2k_B T}{3\mu} (d_i + d_j) \left( \frac{C_i}{d_i} + \frac{C_j}{d_j} \right). \quad (2)$$

In the free-molecular regime ( $Kn > 10$ ) (Lee & Chen, 1984):

$$\beta_{ij}^{\text{fm}} = \left( \frac{3}{4\pi} \right)^{1/6} \left( \frac{6k_B T}{\rho_p} \right)^{1/2} (v_i^{1/3} + v_j^{1/3})^2 \sqrt{\frac{1}{v_i} + \frac{1}{v_j}}. \quad (3)$$

In the transition regime ( $1 < Kn \leq 10$ ) (Fuchs, 1964):

$$\beta_{ij}^{\text{tr}} = 2\pi(d_i + d_j)(D_i + D_j) \left( \frac{d_i + d_j}{d_i + d_j + 2(g_i^2 + g_j^2)^{1/2}} + \frac{8(D_i + D_j)}{(d_i + d_j)(\bar{c}_i^2 + \bar{c}_j^2)^{1/2}} \right)^{-1}, \quad (4)$$

where

$$C_i = 1 + \frac{\lambda}{d_i} \left[ 2.493 + 0.84 \exp \left( \frac{-0.435d_i}{\lambda} \right) \right], \quad (5)$$

$$\bar{c}_i = \left( \frac{8k_B T}{\pi m_i} \right)^{1/2}, \quad (6)$$

$$g_i = \frac{1}{3d_i l_i} [(d_i + l_i)^3 - (d_i^2 + l_i^2)^{3/2}] - d_i, \quad (7)$$

$$l_i = \frac{8D_i}{\pi \bar{c}_i}, \quad (8)$$

$$D_i = \frac{k_B T}{3\pi\mu d_i} \left[ \frac{5 + 4Kn_i + 6Kn_i^2 + 18Kn_i^3}{5 - Kn_i + (8 + \pi)Kn_i^2} \right]. \quad (9)$$

In Eqs. (2)–(9),  $k_B$  is the Boltzmann constant;  $T$  is the absolute temperature;  $\mu$  is the gas viscosity,  $\rho_p$  is the particle density;  $C_i$  is the Stokes–Cunningham slip correction factor for considering the slippage of gas molecules around particle  $i$ ;  $D_i$  is the diffusion coefficient for particle  $i$ ;  $\bar{c}_i$  is the velocity of particle  $i$ ,  $g_i$  is the transition parameter of particle  $i$ .

The numerical solution of the bivariate PBE (Eq. (1)) is generally very challenging due to the double integral and nonlinear behavior of the equation. There are several analytical solutions for the two-component coagulation under considerable simplifications of coagulation kernels (e.g., constant (Gelbard & Seinfeld, 1978; Laurenzi, Bartels, & Diamond, 2002; Lushnikov, 1976), sum (Fernandez-Diaz & Gomez-Garcia, 2007; Laurenzi et al., 2002), and product (Laurenzi et al., 2002)) and initial compositional distributions (e.g., an initially monodisperse distribution of each component or an initially exponential distribution of each component). However, once Brownian coagulation kernels for real processes are considered, there exists no analytical solution for two-component systems and, worse still, the inability of conventional numerical methods makes it difficult to simulate the detailed evolution of compositional distributions. A noteworthy work in this field was contributed by Matsoukas, Lee, and Kim (2006), and Lee, Kim, Rajniak, and Matsoukas (2008). They built up theoretical models to obtain the rate and degree of two-component aggregative mixing as a function of aggregate size and time; and they also used constant-number Monte Carlo method to solve the two-component PBE for Brownian coagulation kernels in the continuum regime and in the free-molecular regime, respectively. Their theoretical models and numerical approaches could be used to determine the distribution of components within aggregates, to quantify the degree of mixing, and to optimize blending of components. Nevertheless, some basic features of the mixing process of two-component Brownian coagulation, especially in the transition regime, are still unresolved; furthermore, the constant-number method demonstrates undesirable statistical noise in compositional distributions and is not able to track the compositional distributions over the full spectrum, in part due to the methodological nature that uses equally weighted simulation particles but also due to the methodological scheme that does not specify how the simulation particles should be distributed over the size and compositional spectra. Thus, it is highly necessary to use robust numerical methods to investigate two-component Brownian coagulation in the three regimes and to provide insight into some characteristics inherent to Brownian aggregative mixing of two components.

We have proposed a differentially weighted Monte Carlo (DWMC) method (Zhao, Kruis, & Zheng, 2010) for two-component coagulation processes, which has been proven to be efficient and precise. Different from conventional MC methods, the DWMC method tracks differentially weighted simulation particles on the basis of a new probabilistic rule for coagulation between two differentially weighted simulation particles, and adopts a component-dependent shift action to restrict the number of simulation particles for each size interval of each component space within prescribed bounds during simulation. This paper briefly introduces the DWMC method and then utilizes it to simulate the two-component Brownian coagulation.

## 2. Differentially weighted Monte Carlo (DWMC) method for two-component coagulation

When simulating two or more internal variables of particles (e.g., in this paper, two chemical compositions), conventional deterministic methods such as the method of moments (McGraw & Wright, 2003) and sectional method (Kim & Seinfeld, 1990) are formulated by complicated mathematical equations, but could not deal with the innate fluctuations for multi-component coagulation (Laurenzi et al., 2002). And more unfortunately, the conventional deterministic methods may not be valid for long time periods, when only several particles acquire enough mass to become larger than that of the rest of the population (Alfonso, Raga, & Baumgardner, 2008) for complete coagulation to occur (Laurenzi et al., 2002). Fortunately, stochastic methods (Kruis, Maisels, & Fissan, 2000; Lee et al., 2008; Maisels, Kruis, & Fissan, 2002; Matsoukas et al., 2006; Sun, Axelbaum, & Huertas, 2004), which directly simulate the dynamic evolution of a finite sample of the particle population using Monte Carlo (MC) technique, are capable of simulating multi-component population balances in a simple and straightforward manner.

We have proposed the DWMC method for particle coagulation in monovariate systems (Zhao, Kruis, & Zheng, 2009; Zhao & Zheng, 2009), and then extended it to two-component coagulation processes (Zhao et al., 2010). The robust MC is briefly presented as follows:

- (1) Simulation particles are differentially weighted according to initial compositional distributions. First, two individual compositional spectra are respectively divided into intervals by laws which can be freely adapted to the problems to be solved, to result in a sectionalized two-dimensional space of compositional distribution. With respect to a section  $(p, q)$  in the space, it represents a state  $(v_{x,p}, v_{y,q})$  of particles having  $x$ -component volumes between  $v_{x,p}^-$  and  $v_{x,p}^+$  and  $y$ -component volumes between  $v_{y,q}^-$  and  $v_{y,q}^+$ , and the number concentration of these particles is  $n(v_{x,p}, v_{y,q}, 0)(v_{x,p}^+ - v_{x,p}^-)(v_{y,q}^+ - v_{y,q}^-)$ . These real particles are considered to have similar dynamic behavior and are represented by a certain number of weighted simulation particles. The mean weight of simulation particles for section  $(p, q)$  is thus calculated as:

$$\bar{w}_{pq}(v_{x,p}, v_{y,q}) = \frac{n(v_{x,p}, v_{y,q}, 0)(v_{x,p}^+ - v_{x,p}^-)(v_{y,q}^+ - v_{y,q}^-)V}{N_s(v_{x,p}, v_{y,q})}, \quad (10)$$

where  $N_s(v_{x,p}, v_{y,q})$  is the number of simulation particles located at section  $(p, q)$ ,  $V$  is the volume of the simulated system. In the DWMC method,  $N_s$  is prescribed to be more than a fixed minimum number  $N_{s,\min}$  but less than a maximum number  $N_{s,\max}$ .

cles having larger weight values than sections where number density is low.

- (2) An adjustable time step is determined from local mean-field coagulation rate:

$$\Delta t = \frac{pN_{st}}{\sum_{i=1}^{N_{st}} (VC'_i)}, \quad (11)$$

where empirical parameter  $p$  is set around  $2/N_{st} - 0.05$ ;  $N_{st}$  is the total number of simulation particles in the system;  $C'_i$  (with unit of  $\text{m}^{-3} \text{s}^{-1}$ ) is the total coagulation rate of simulation particle  $i$ .  $C'_i$  is calculated from the probabilistic coagulation rule for coagulation event between two differentially weighted simulation particles (Zhao et al., 2009; Zhao & Zheng, 2009). In this rule, for a coagulation event between simulation particles  $i$  and  $j$ , it is imagined that each real particle from  $i$  undergoes a real coagulation event with a probability of  $\min(w_i, w_j)/w_i$ , and each real particle from  $j$  does so with a probability of  $\min(w_i, w_j)/w_j$ , where  $w_i$  and  $w_j$  are the private weights of  $i$  and  $j$ , respectively.  $C'_i$  is thus calculated as

$$C'_i = \frac{1}{V^2} \sum_{j=1, j \neq i}^{N_{st}} \left[ \frac{2\beta_{ij}w_j \max(w_i, w_j)}{w_i + w_j} \right] = \frac{1}{V^2} \sum_{j=1, j \neq i}^{N_{st}} \beta'_{ij}, \quad (12)$$

where  $\beta_{ij}$  is the coagulation kernel between particle  $i$  and particle  $j$ ,  $\text{m}^3/\text{s}$ ;  $\beta'_{ij}$  is a normalized kernel that relates not only to the states (like volumes) but also to the weights of the two simulation particles.

It is noteworthy that DWMC evolves in either event-driven mode or time-driven mode according to the value of empirical parameter  $p$ . If  $p = 2/N_{st}$ , the resultant time-step,  $2/(V \sum_{i=1}^{N_{st}} C'_i)$ , is just the waiting time between two successive coagulation events, and DWMC evolves in the event-driven mode, where only one coagulation event occurs within this time-step. If  $p > 2/N_{st}$ , there are  $pN_{st}/2$  coagulation events within the time-step and DWMC evolves in the time-driven mode. Generally speaking, the event-driven version is more accurate because events are fully uncoupled among different time steps, while the time-driven mode is faster because many events are simulated within one time step.

- (3) Within the time step the interacting particle pair(s) is (are) selected with probability  $\beta'_{ij}/\sum_i \sum_{j, j \neq i} \beta'_{ij}$ . Either the cumulative probability method or the acceptance-rejection method is adopted to determine coagulated pair(s) in either event-driven mode or time-driven mode, as described in reference (Zhao et al., 2010).
- (4) The coagulation event between interacting pair results in new simulation particles with new states and weights according to the probabilistic coagulation rule. As for the  $i$ - $j$  coagulation event, two new simulation particles replace the “old” particles  $i$  and  $j$ , as formulated by:

$$\begin{aligned} & \text{if } w_i \neq w_j, \quad \begin{cases} w_i^* = \max(w_i, w_j) - \min(w_i, w_j), & m_i^* = m_k |_{w_k = \max(w_i, w_j)}, & v_i^* = v_k |_{w_k = \max(w_i, w_j)}, \\ v_{x,i}^* = v_{x,k} |_{w_k = \max(w_i, w_j)}, & v_{y,i}^* = v_{y,k} |_{w_k = \max(w_i, w_j)}, \\ w_j^* = \min(w_i, w_j), & m_j^* = m_i + m_j, & v_j^* = v_i + v_j, \\ v_{x,j}^* = v_{x,i} + v_{x,j}, & v_{y,j}^* = v_{y,i} + v_{y,j}, \end{cases} \\ & \text{if } w_i = w_j, \quad \begin{cases} w_i^* = \frac{w_i}{2}, & m_i^* = m_i + m_j, & v_i^* = v_i + v_j, \\ v_{x,i}^* = v_{x,i} + v_{x,j}, & v_{y,i}^* = v_{y,i} + v_{y,j}, \\ w_j^* = \frac{w_j}{2}, & m_j^* = m_i + m_j, & v_j^* = v_i + v_j, \\ v_{x,j}^* = v_{x,i} + v_{x,j}, & v_{y,j}^* = v_{y,i} + v_{y,j}, \end{cases} \end{aligned} \quad (13)$$

Sections where number density of real particles is high can thus be designated to have a certain number of simulation parti-

cles where the asterisk indicates a new value of weight or state after the coagulation event;  $m_i$  and  $v_i$  are the total mass and volume

of simulation particle  $i$ ;  $v_{x,i}$  and  $v_{y,i}$  are the mass of component  $x$  and component  $y$  in simulation particle  $i$ . It is obvious that Eq. (13) satisfies the law of conservation of mass, and DWMC is capable of keeping simulation particle number constant. Particle diameter  $d$  is obtained from particle volume, provided that the aggregates are spherical due to faster sintering in high temperature.

- (5) The total coagulation rate of each particle is updated according to the involved coagulation event(s) within  $\Delta t$  using the smart-bookkeeping technique (Zhao et al., 2009).
- (6) When certain conditions are reached, for example, when the number concentration of real particles is halved, the composition-dependent shift action is performed which restricts the number of simulation particles in predefined size intervals of each component space within these prescribed bounds (between  $N_{s,\min}$  and  $N_{s,\max}$ ). The action is realized as following: first, the distribution of each component is sectionalized by some prescribed laws (e.g., logarithmical discretization) and the number of simulation particles in the chosen intervals of each component space is counted (e.g., the numbers of simulation particles in size interval  $p$  of  $x$ -component space and size interval  $q$  of  $y$ -component space are  $N_{sx,p}$  and  $N_{sy,q}$ , respectively). Then, with respect to a section  $(p,q)$  of the two-component space, if  $\min(N_{sx,p}, N_{sy,q}) < N_{s,\min}$ , a simulation particle  $i$  in the section  $(p,q)$  is equally split into new simulations particles with an integer number  $[N_{s,\min}/\min(N_{sx,p}, N_{sy,q})]$ . These new particles have the same internal variables as their parent particle  $i$  and have a weight of  $w_i/[N_{s,\min}/\min(N_{sx,p}, N_{sy,q})]$ . One daughter particle replaces the position of its parent particle  $i$ , and other daughter particles are added to the array of simulation particles; if  $\max(N_{sx,p}, N_{sy,q}) > N_{s,\max}$ , a simulation particle  $j$  in the section  $(p,q)$  can be randomly removed with a probability of  $[\max(N_{sx,p}, N_{sy,q}) - N_{s,\max}]/\max(N_{sx,p}, N_{sy,q})$ . A random process is used to decide whether simulation particle  $j$  is removed or not. If a random number  $r$  from a uniform distribution in the interval  $[0,1]$  is less than  $[\max(N_{sx,p}, N_{sy,q}) - N_{s,\max}]/\max(N_{sx,p}, N_{sy,q})$ ,  $j$  is removed and its open position is taken by the last particle in the simulation particle array. If not, the number weight of  $j$  is corrected by a multiple factor  $\max(N_{sx,p}, N_{sy,q})/N_{s,\max}$ .

In fact, the action shifts some simulation particles from densely populated regions of the two-dimensional component space to less populated regions by splitting some simulation particles in less populated regions into more simulation particles and randomly removing some simulation particles in densely populated regions from the simulation. The composition-dependent shift action overcomes the drawback of a stochastic approach as far as possible, and at the same time the computational cost can be limited.

- (7) Steps (2)–(6) are repeated until  $\sum \Delta t$  reaches the prescribed end time of process simulation.

The DWMC method is especially effective for two-component coagulation because differentially weighted simulation particles can be specified to distribute as homogeneously as possible over high-dimensional joint space of internal variables, which will greatly reduce statistical noise inherent to the MC method and determine full compositional distributions in multi-component coagulation processes. We utilize the DWMC method to describe two-component Brownian coagulation, which are commonly encountered in industrial processes such as nanoparticle synthesis, coal combustion, incineration, granulation, and crystallization.

### 3. Two-component Brownian coagulation

#### 3.1. Self-preserving distribution

It is well known that the size distribution of mono-component particles satisfies the self-preserving form after a time-lag in cases of Brownian coagulation in the continuum regime or in the free-molecular regime (Friedlander, 2000). In this study, two-component Brownian coagulation processes in the continuum regime, in the free-molecular regime, and in the transition regime are respectively simulated to study whether the compositional distribution in these cases is still self-preserving or not. Although no analytical solution of compositional distribution exists, the discrete-sectional models (Landgrebe & Pratsinis, 1990; Vemury & Pratsinis, 1995) provide classical benchmark solutions of self-preserving particle size distributions for Brownian coagulation in the continuum and free-molecular regimes.

In the self-preserving formulation, the dimensionless particle volume is defined as  $\eta = Nv/M = v/\bar{v}$ , and the dimensional distribution as  $\Psi = Mn(v, t)/N^2$  (Friedlander & Wang, 1966), where  $N$  is the total number concentration of particles,  $M$  is the total mass (or volume) concentration,  $\bar{v}$  is the average volume,  $n(v, t)$  is the particle size distribution function at time  $t$  such that  $n(v, t)dv$  represents the number concentration of particles in the volume range of  $v$  to  $v + dv$ . As for two-component coagulation, the dimensionless volume and number density distribution of  $x$ -component are defined as

$$\eta_x = \frac{N_x v_x}{M_x} = \frac{v_x}{\bar{v}_x}, \quad \Psi_x = \frac{M_x n_x(v_x, t)}{N_x^2}, \quad (14)$$

where  $N_x$  is total number concentration of particles containing  $x$ -component (in the case, there may be some particles not containing  $x$ -component due to the initial discrete distribution, thus  $N_x$  may be unequal to  $N$ );  $M_x$  is total mass concentration of  $x$ -component (it may not be equal to the total mass concentration of particles);  $\bar{v}_x$  is the average  $x$ -component volume; and  $n_x(v_x, t)$  is the number density distribution function of  $x$ -component at time  $t$  such that  $n_x(v_x, t)dv_x$  represents the number concentration of particles in the  $x$ -component volume range of  $v_x$  to  $v_x + dv_x$ . Similarly:

$$\eta_y = \frac{N_y v_y}{M_y} = \frac{v_y}{\bar{v}_y}; \quad \Psi_y = \frac{M_y n_y(v_y, t)}{N_y^2}. \quad (15)$$

The dimensionless distribution is obviously subjected to the integral constraints:

$$\begin{aligned} \int_0^\infty \Psi d\eta &= 1, & \int_0^\infty \eta \Psi d\eta &= 1, \\ \int_0^\infty \Psi_x d\eta_x &= 1, & \int_0^\infty \eta_x \Psi_x d\eta_x &= 1, \\ \int_0^\infty \Psi_y d\eta_y &= 1, & \int_0^\infty \eta_y \Psi_y d\eta_y &= 1. \end{aligned} \quad (16)$$

The characteristic coagulation time scales for the three Brownian coagulation cases are defined as follows:

In the free-molecular regime:

$$\tau_{\text{coag}}^{\text{fm}} = \left[ \left( \frac{3k_B T d_0}{\rho_p} \right)^{1/2} \left( \frac{3}{4\pi} \right)^{1/6} N_0 \right]^{-1}. \quad (17)$$

In the continuum regime:

$$\tau_{\text{coag}}^{\text{co}} = \frac{3\mu}{2k_B T N_0}. \quad (18)$$

In the transition regime:

$$\tau_{\text{coag}}^{\text{tr}} = \frac{1}{\beta^{\text{tr}}(d_{x0}, d_{y0}) N_0}. \quad (19)$$



**Table 1**  
Simulation conditions for three two-component Brownian coagulation cases (per unit volume of computational domain).

Coagulation case	$N_{x0}$ (m <sup>-3</sup> )	$N_{y0}$ (m <sup>-3</sup> )	$d_{x0}$ (μm)	$d_{y0}$ (μm)	$T$ (K)	$\mu$ (Pa·s)	$\rho_p$ (kg/m <sup>3</sup> )
In continuum regime	$3 \times 10^{21}$	$7 \times 10^{21}$	0.5	0.5	300	$1.81 \times 10^{-5}$	–
In free-molecular regime	$7 \times 10^{21}$	$3 \times 10^{21}$	0.001	0.002	1800	–	4200
In transition regime	$4 \times 10^{21}$	$6 \times 10^{21}$	0.02	0.01	1800	$5.65 \times 10^{-5}$	4200

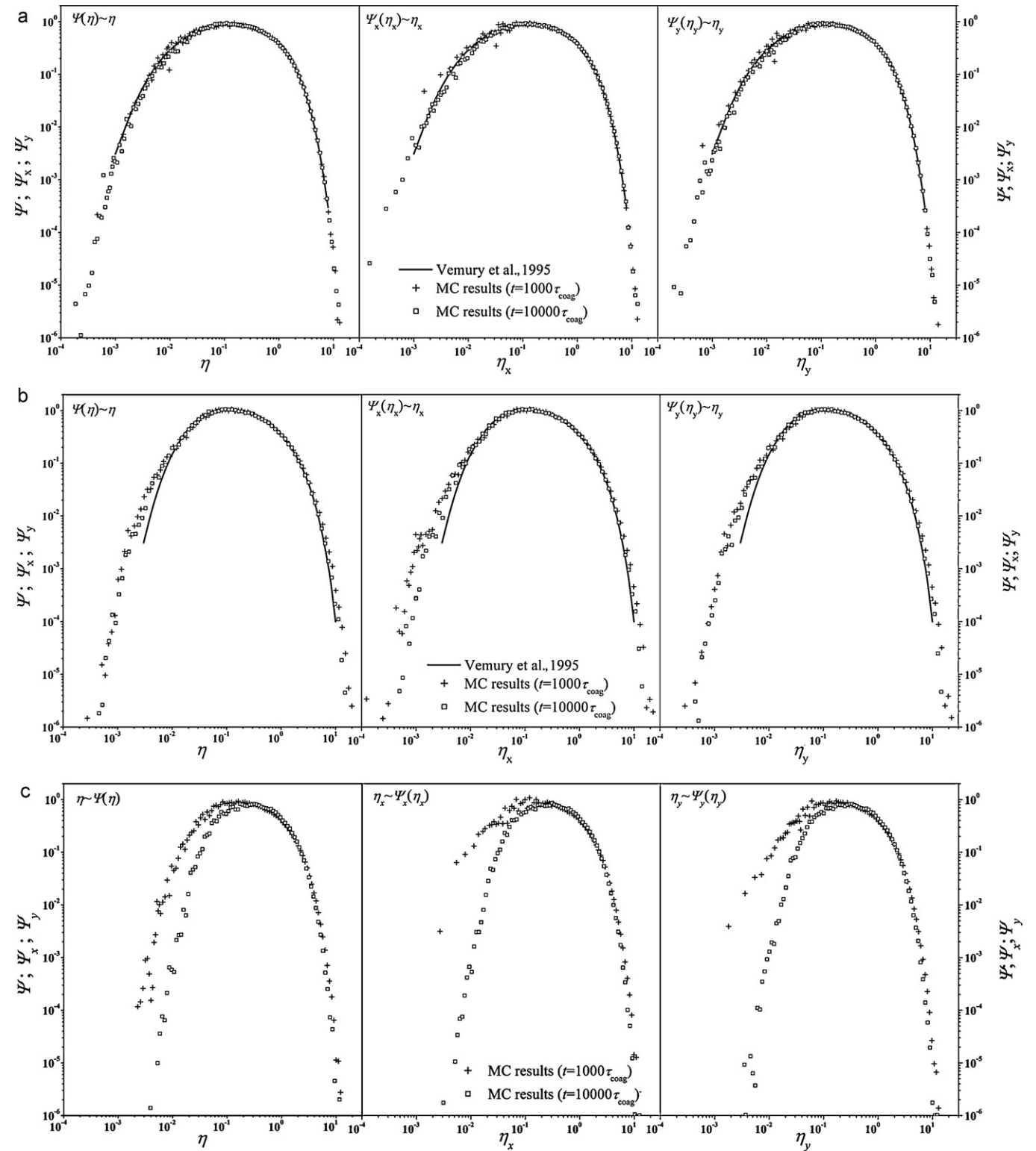


**Fig. 1.** Self-preserving size distribution and mono-variate compositional distributions for two-component Brownian coagulation. (a) In the continuum regime:  $N_{x0}:N_{y0} = 3:7$ ,  $\nu_{x0}:\nu_{y0} = 1:1$ ; (b) in the free-molecular regime:  $N_{x0}:N_{y0} = 7:3$ ,  $\nu_{x0}:\nu_{y0} = 1:8$ ; and (c) in the transition regime:  $N_{x0}:N_{y0} = 4:6$ ,  $\nu_{x0}:\nu_{y0} = 8:1$ .

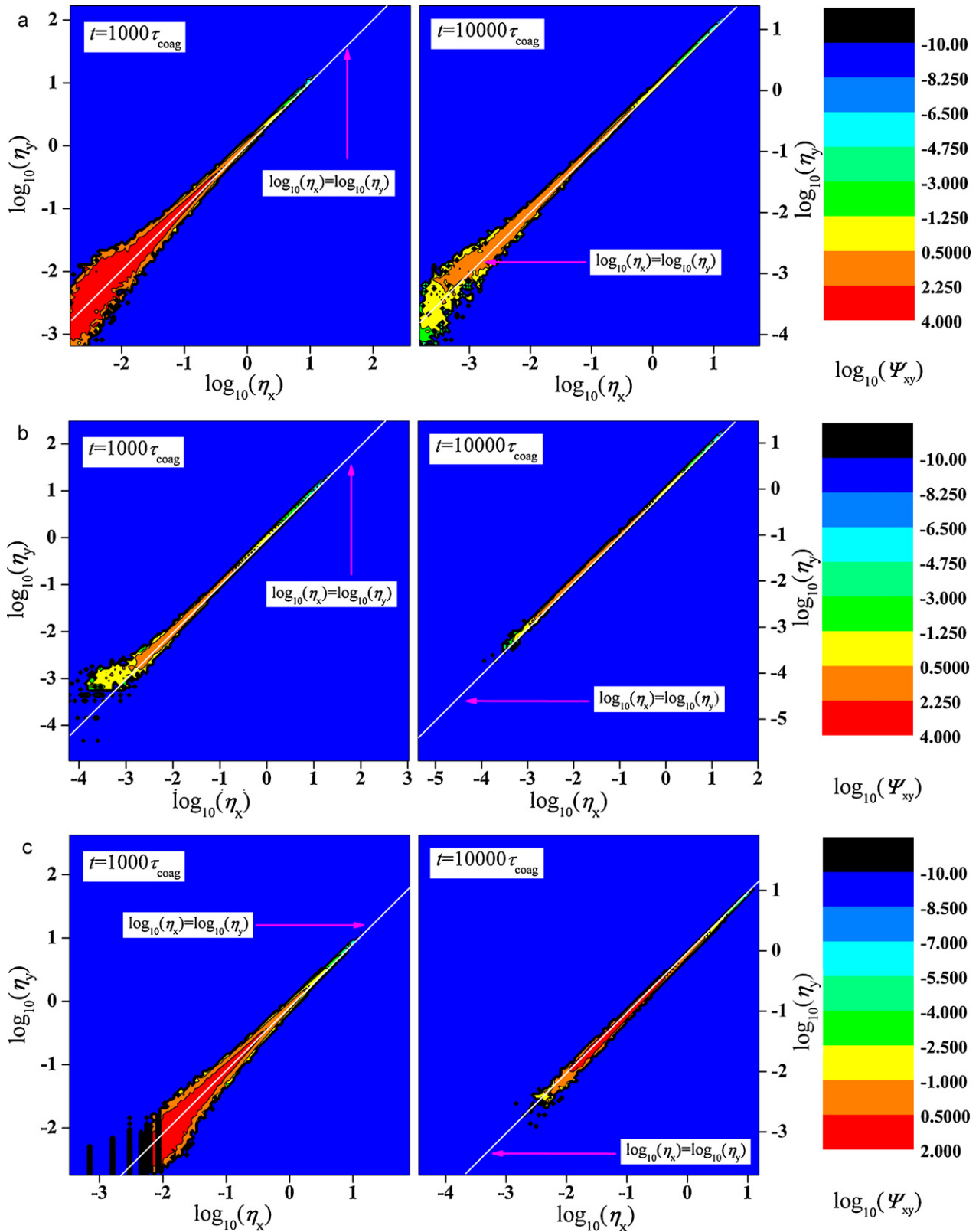


**Fig. 2.** The dimensionless bivariate compositional distributions at different time points. (a) in the continuum regime; (b) in the free-molecular regime; and (c) in the transition regime.

With respect to any simulation, each particle has only one chemical component at the initial stage, either  $x$ -component or  $y$ -component. The detailed simulation conditions for three two-component Brownian coagulation cases are listed in Table 1.

Fig. 1(a)–(c) shows the dimensionless particle size distribution and dimensionless mono-variate compositional distributions (the number density distribution function of one component amount, in the form of volume of the component in aggregates) for Brownian

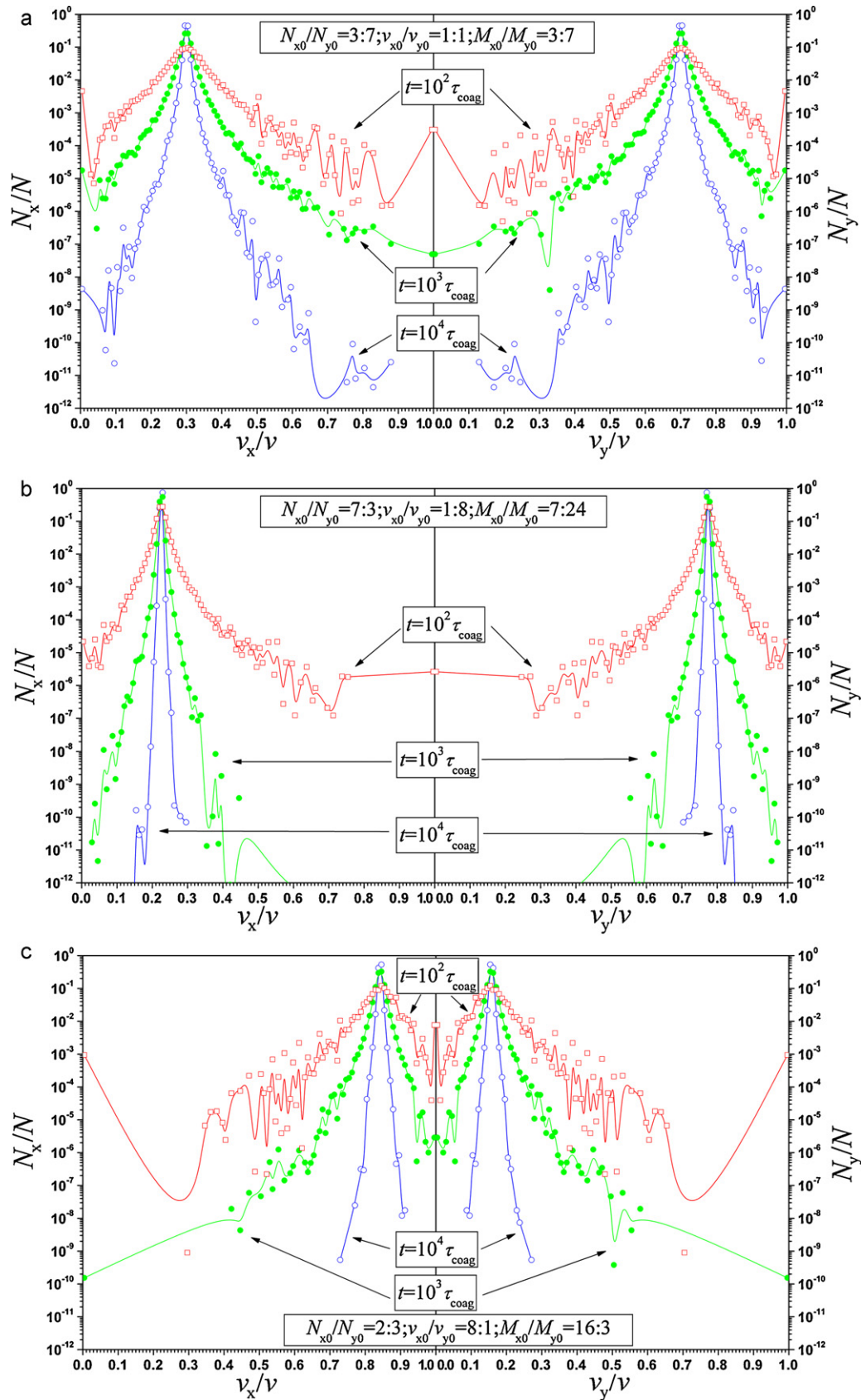


**Fig. 3.** Compositional number density distributions for two-component Brownian coagulation. (a) In the continuum regime:  $N_{x0}:N_{y0} = 3:7$ ,  $v_{x0}:v_{y0} = 1:1$ ,  $M_{x0}:M_{y0} = 3:7$ ; (b) in the free-molecular regime:  $N_{x0}:N_{y0} = 7:3$ ,  $v_{x0}:v_{y0} = 1:8$ ,  $M_{x0}:M_{y0} = 7:24$ ; and (c) in the transition regime:  $N_{x0}:N_{y0} = 2:3$ ,  $v_{x0}:v_{y0} = 8:1$ ,  $M_{x0}:M_{y0} = 16:3$ .

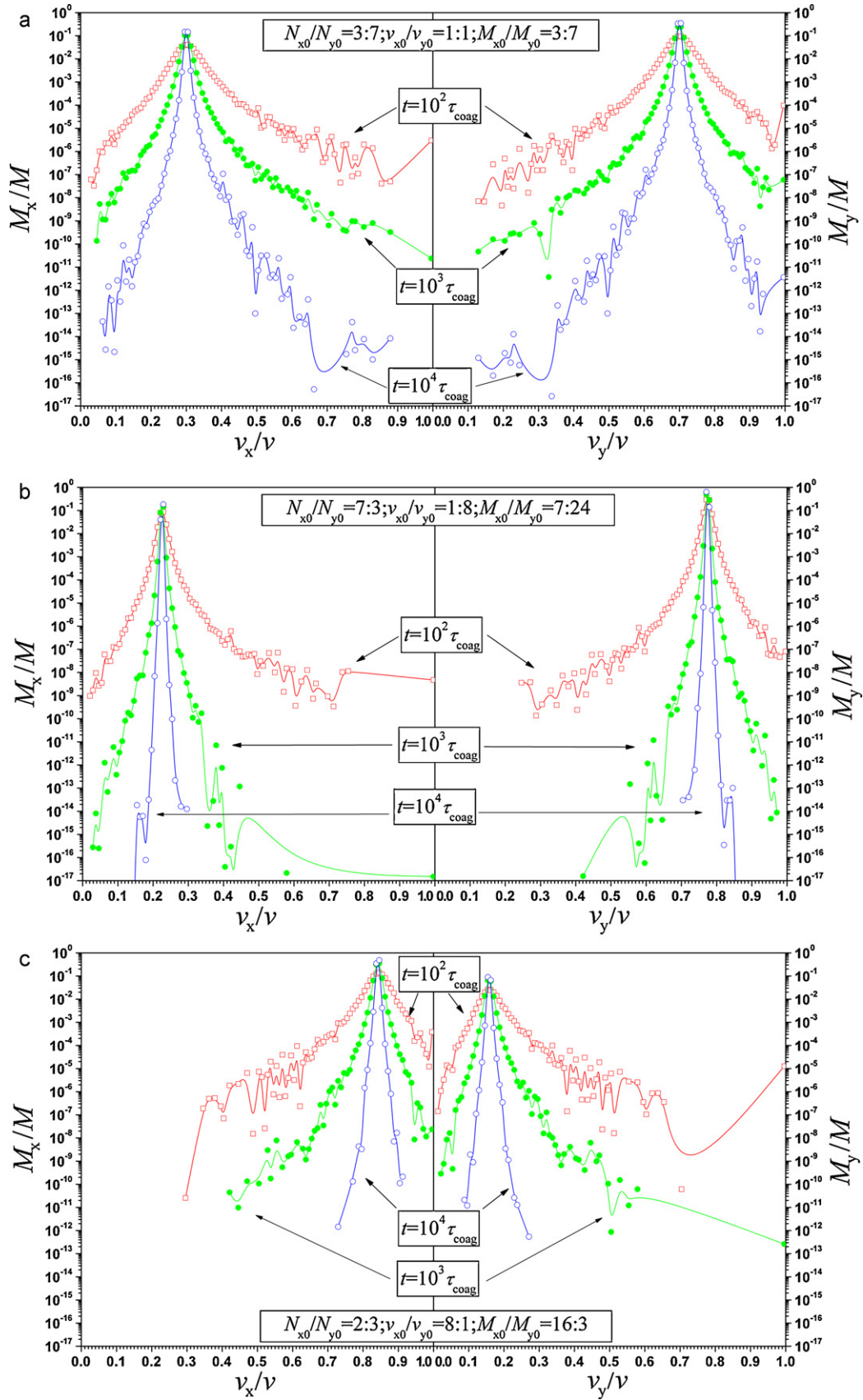


**Fig. 4.** Compositional mass density distributions for two-component Brownian coagulation. (a) In the continuum regime:  $N_{x0}:N_{y0} = 3:7$ ,  $v_{x0}:v_{y0} = 1:1$ ,  $M_{x0}:M_{y0} = 3:7$ ; (b) in the free-molecular regime:  $N_{x0}:N_{y0} = 7:3$ ,  $v_{x0}:v_{y0} = 1:8$ ,  $M_{x0}:M_{y0} = 7:24$ ; and (c) in the transition regime:  $N_{x0}:N_{y0} = 2:3$ ,  $v_{x0}:v_{y0} = 8:1$ ,  $M_{x0}:M_{y0} = 16:3$ .



**Table 2**

Peak values of compositional number (and mass) density distribution.

	In continuum regime			In free-molecular regime			In transition regime		
	$t = 10^2 \tau_{\text{coag}}$	$t = 10^3 \tau_{\text{coag}}$	$t = 10^4 \tau_{\text{coag}}$	$t = 10^2 \tau_{\text{coag}}$	$t = 10^3 \tau_{\text{coag}}$	$t = 10^4 \tau_{\text{coag}}$	$t = 10^2 \tau_{\text{coag}}$	$t = 10^3 \tau_{\text{coag}}$	$t = 10^4 \tau_{\text{coag}}$
$\max(N_x/N)$	0.0957	0.2612	0.4528	0.2781	0.5506	0.7510	0.1194	0.3268	0.5369
$\max(N_y/N)$	0.0941	0.2606	0.4534	0.2780	0.5506	0.7510	0.1193	0.3269	0.5369
$\max(N_x/N):\max(N_y/N)$	1.0170	1.0023	0.9987	1.0001	1.0000	1.0000	1.0003	0.9994	1.0000
$(v_x/v)/(\max(N_x/N))$	0.3042	0.3042	0.2958	0.2292	0.2292	0.2292	0.8458	0.8458	0.8458
$(v_y/v)/(\max(N_y/N))$	0.7042	0.7042	0.7042	0.7708	0.7708	0.7708	0.1542	0.1542	0.1542
$\{(v_x/v)/(\max(N_x/N))\}:\{(v_y/v)/(\max(N_y/N))\}$	0.4320	0.4320	0.4320	0.2973	0.2973	0.2973	5.4863	5.4863	5.4863
$\max(M_x/M)$	0.0410	0.1055	0.1478	0.0873	0.1415	0.1851	0.1397	0.3545	0.4858
$\max(M_y/M)$	0.0948	0.2439	0.3484	0.2945	0.4826	0.6341	0.0256	0.0649	0.0901
$\max(M_x/M):\max(M_y/M)$	0.4325	0.4326	0.4242	0.2963	0.2932	0.2918	5.4693	5.4586	5.3939
$(v_x/v)/(\max(M_x/M))$	0.3042	0.3042	0.2958	0.2292	0.2292	0.2292	0.8458	0.8458	0.8458
$(v_y/v)/(\max(M_y/M))$	0.7042	0.7042	0.7042	0.7708	0.7708	0.7708	0.1542	0.1542	0.1542
$\{(v_x/v)/(\max(M_x/M))\}:\{(v_y/v)/(\max(M_y/M))\}$	0.4320	0.4320	0.4320	0.2973	0.2973	0.2973	5.4863	5.4863	5.4863

coagulation in the three regimes, respectively. It is found that not only the size distribution ( $\Psi$  vs  $\eta$ ) but also the mono-variate compositional distributions ( $\Psi_x$  vs  $\eta_x$  and  $\Psi_y$  vs  $\eta_y$ ) are self-preserving forms for Brownian coagulation cases in the continuum regime and in the free-molecular regime. Also, both the size distribution and the mono-variate compositional distributions correspond to the same self-similar formulation for the two cases. However, the size distribution and the mono-variate compositional distributions in the transition regime cannot reach the self-preserving form, as expected in the mono-component Brownian coagulation in the transition regime.

With respect to the combined number density distribution of  $x$ -component and  $y$ -component (the bivariate compositional distribution), its dimensionless form is defined as

$$\Psi_{xy} = \frac{M_x M_y n(v_x, v_y, t)}{N_x N_y N_{xy}}, \quad (20)$$

where  $N_{xy}$  (with unit of  $\text{m}^{-3}$ ) is total number concentration of particles simultaneously containing  $x$ -component and  $y$ -component,  $M_{xy}$  (with unit of  $\text{m}^3 \times \text{m}^3 \times \text{m}^{-3}$ ) is total mass concentration of particles simultaneously containing  $x$ -component and  $y$ -component, and  $\bar{v}_{xy} = M_{xy}/N_{xy} = M_{1,1}/M_{0,0}$ . It is found that

$$\int_0^\infty \int_0^\infty \Psi_{xy} d\eta_x d\eta_y = 1, \quad \int_0^\infty \int_0^\infty \eta_x \eta_y \Psi_{xy} d\eta_x d\eta_y = \frac{M_{xy} N_x N_y}{N_{xy} M_x M_y} = \frac{\bar{v}_{xy}}{\bar{v}_x \bar{v}_y} \neq 1. \quad (21)$$

Obviously, the dimensionless bivariate compositional distribution does not satisfy the normalizing condition and is thus not self-preserving from the classical Friedlander's point of view (Friedlander, 2000). However, from the dimensionless bivariate distribution at different time points, as shown in Fig. 2, we can find that the contour plot of the logarithm of the normalized two-dimensional compositional distribution function,  $\log_{10}(\Psi_{xy})$ , is nearly symmetric about the line  $\log_{10}(\eta_y) = \log_{10}(\eta_x)$  on the plane  $\log_{10}(\eta_y) - \log_{10}(\eta_x)$ . The white line in the three sub-figures represents the line  $\log_{10}(\eta_y) = \log_{10}(\eta_x)$ . Rather, as time evolves,  $\log_{10}(\Psi_{xy})$  stretches along with the line  $\log_{10}(\eta_y) = \log_{10}(\eta_x)$ , resulting in a slimmer and slimmer contour plot. We thus argue that the bivariate compositional distribution satisfies a semi self-preserving form for Brownian coagulation cases in the continuum regime, in the free-molecular regime, and also in the transition regime.

We also simulated the coagulation processes of two-component systems having different initial component distributions, for example, different  $N_{x0}:N_{y0}$  and  $v_{x0}:v_{y0}$ . Similar results, which are not shown here because of limited space, are obtained for the three Brownian coagulation cases. It is worth emphasizing that not only the self-preserving size distribution and mono-variate compositional

distributions (like Fig. 1) but also the semi self-preserving bivariate compositional distributions (like Fig. 2) are independent of initial compositional distributions.

### 3.2. Aggregative mixing

With respect to the three two-component Brownian coagulation cases described in Section 3.1, Fig. 3 shows the mono-variate compositional distribution in terms of the compositional number density distribution ( $N_x/N$  or  $N_y/N$ ) vs. the component mass ratio ( $v_x/v$  or  $v_y/v$ ) at several representative time points. The corresponding compositional mass density distribution ( $M_x/M$  or  $M_y/M$ ) against the component mass ratio is plotted in Fig. 4. The first direct observation from Fig. 3 is that the number density distribution of  $x$ -component closely mirrors the number density distribution of  $y$ -component. The simulation results obviously meet the intuitive understanding of aggregative mixing of the two-component system. The excellent mirror should be ascribed to that the differentially weighted MC is capable of capturing the details of not only the homogeneously mixed particles, which occupy a larger number (and mass) share in particle population (for example, the particles whose  $v_x/v_y$  is 3:7), but also the inhomogeneously mixed particles, which are much less-populated (for example, the particles at the two edges of compositional distributions). We also observe that the geometric standard deviation of both  $x$ -component and  $y$ -component number (and mass) density distributions decreases as time evolves, that is, as aggregate size increases. The results show the degree of mixing between components improves as aggregate size increases, much in agreement with the numerical simulation and theoretical predictions of Matsoukas et al. (2006) and Lee et al. (2008).

The peak of component number (and mass) density distribution calls for particular attention, as shown by the maximum values of  $N_x/N$  (or  $N_y/N$ ) and  $M_x/M$  (or  $M_y/M$ ) as well as the corresponding  $v_x/v$  (or  $v_y/v$ ) listed in Table 2. It is found that the component number (and mass) density distributions are peaked at the corresponding mass fraction of  $x$ -component  $\Phi_x = M_{x0}/(M_{x0} + M_{y0})$ , and  $\Phi_y = M_{y0}/(M_{x0} + M_{y0})$  when reaching the self-preserving size and/or compositional distributions, implying that the two-component mixing is largely controlled by the initial degree of segregation in the feed. These results also agree with those of Matsoukas et al. (2006), and Lee et al. (2008). It is interesting that  $\max(N_x/N):\max(N_y/N)$  at different moments is approximately equal to 1:1 and  $\max(M_x/M):\max(M_y/M)$  approaches  $\Phi_x:\Phi_y$  (3:7=0.4286 for the coagulation case in the continuum regime, 7:24=0.2917 for the case in the free-molecular regime, and 16:3=5.3333 for the case in the transition regime). And, as aggregate size increases the maximum values of  $N_x/N$  (or  $N_y/N$ ) and  $M_x/M$

(or  $M_y/M$ ) increase accordingly. The above observations also hold in other cases where the initial size and number of two components are different, and are also true for two-component Brownian coagulation in the continuum regime, in the free-molecular regime, also in the transition regime.

#### 4. Conclusions

The two-component Brownian coagulation is simulated by the differentially weighted MC method. It is found that: (1) the self-preserving formulations of both size distribution and mono-variate compositional distributions are obtained for Brownian coagulation cases in the continuum regime and in the free-molecular regime, where the values of the self-preserving mono-variate compositional distributions are the same as those of the self-preserving size distributions; however Brownian coagulation in transition regime cannot reach self-preserving size distribution and mono-variate compositional distributions. (2) The bivariate compositional distribution of two components satisfies a semi self-preserving form for any Brownian coagulation case, that is, the normalized two-dimensional compositional distribution is symmetrically distributed independent of initial compositional distributions; (3) the degree of mixing between components improves (i.e., the width of the compositional distributions is narrower and narrower) as aggregate size increases; (4) the compositional number (and mass) density distribution is largely controlled by the initial compositional mass fraction.

#### Acknowledgements

H. Zhao was supported by funds from “The National Natural Science Foundation of China” (50876037 and 50721005), “Program for New Century Excellent Talents in University” (NCET-10-0395), and “National Key Basic Research and Development Program” (2010CB227004).

#### References

- Alfonso, L., Raga, G. B., & Baumgardner, D. (2008). Monte Carlo simulations of two-component drop growth by stochastic coalescence. *Atmospheric Chemistry and Physics Discussions*, 8(2), 7289–7313.
- Fernandez-Diaz, J. M., & Gomez-Garcia, G. J. (2007). Exact solution of Smoluchowski's continuous multi-component equation with an additive kernel. *Europhysics Letters*, 78(5), 56002.
- Friedlander, S. K. (2000). *Smoke, dust and haze: Fundamentals of aerosol dynamics* (2nd ed.). New York: Oxford University Press.
- Friedlander, S. K., & Wang, C. S. (1966). The self-preserving particle size distribution for coagulation by Brownian motion. *Journal of Colloid and Interface Science*, 22(2), 126–132.
- Fuchs, N. A. (1964). *The mechanics of aerosols*. New York: Pergamon Press.
- Gelbard, F. M., & Seinfeld, J. H. (1978). Coagulation and growth of a multicomponent aerosol. *Journal of Colloid and Interface Science*, 63(3), 472–479.
- Kim, Y. P., & Seinfeld, J. H. (1990). Simulation of multicomponent aerosol condensation by the moving sectional method. *Journal of Colloid and Interface Science*, 135(1), 185–199.
- Kruis, F. E., Maisels, A., & Fissan, H. (2000). Direct simulation Monte Carlo method for particle coagulation and aggregation. *AIChE Journal*, 46(9), 1735–1742.
- Landgrebe, J. D., & Pratsinis, S. E. (1990). A discrete-sectional model for particulate production by gas-phase chemical reaction and aerosol coagulation in the free-molecular regime. *Journal of Colloid and Interface Science*, 139(1), 63–86.
- Laurenzi, I. J., Bartels, J. D., & Diamond, S. L. (2002). A general algorithm for exact simulation of multicomponent aggregation processes. *Journal of Computational Physics*, 177(2), 418–449.
- Lee, K. W., & Chen, H. (1984). Coagulation rate of polydisperse particles. *Aerosol Science & Technology*, 3(3), 327–334.
- Lee, K., Kim, T., Rajniak, P., & Matsoukas, T. (2008). Compositional distributions in multicomponent aggregation. *Chemical Engineering Science*, 63(5), 1293–1303.
- Lushnikov, A. A. (1976). Evolution of coagulating systems: III. Coagulating mixtures. *Journal of Colloid and Interface Science*, 54(1), 94–101.
- Maisels, A., Kruis, F. E., & Fissan, H. (2002). Mixing selectivity in bicomponent, bipolar aggregation. *Journal of Aerosol Science*, 33(1), 35–49.
- Matsoukas, T., Lee, K., & Kim, T. (2006). Mixing of components in two-component aggregation. *AIChE Journal*, 52(9), 3088–3099.
- McGraw, R., & Wright, D. L. (2003). Chemically resolved aerosol dynamics for internal mixtures by the quadrature method of moments. *Journal of Aerosol Science*, 34, 189–209.
- Pratsinis, S. E. (1998). Flame aerosol synthesis of ceramic powders. *Progress in Energy and Combustion Science*, 24(3), 197–219.
- Sun, Z., Axelbaum, R., & Huertas, J. (2004). Monte Carlo simulation of multicomponent aerosols undergoing simultaneous coagulation and condensation. *Aerosol Science and Technology*, 38(10), 963–971.
- Vemury, S., & Pratsinis, S. E. (1995). Self-preserving size distributions of agglomerates. *Journal of Aerosol Science*, 26, 175–185.
- Zhao, H., Kruis, F. E., & Zheng, C. (2009). Reducing statistical noise and extending the size spectrum by applying weighted simulation particles in Monte Carlo simulation of coagulation. *Aerosol Science and Technology*, 43(8), 781–793.
- Zhao, H., Kruis, F. E., & Zheng, C. A. (2010). A differentially weighted Monte Carlo method for two-component coagulation. *Journal of Computational Physics*, 229(19), 6931–6945.
- Zhao, H., & Zheng, C. (2009). A new event-driven constant-volume method for solution of the time evolution of particle size distribution. *Journal of Computational Physics*, 228(5), 1412–1428.